New Insights on the Distribution of Interlayer Water in Bi-Hydrated Smectite from X-ray Diffraction Profile Modeling of 00 l Reflections

ARTICLE *in* CHEMISTRY OF MATERIALS · JUNE 2005

Impact Factor: 8.35 · DOI: 10.1021/cm047995v

6 AUTHORS, INCLUDING:

Eric Ferrage
Université de Poitiers
57 PUBLICATIONS **1,194** CITATIONS
SEE PROFILE

Bruno Lanson
CNRS / Univ. Grenoble Alpes
105 PUBLICATIONS **3,530** CITATIONS
SEE PROFILE

Natalie Malikova
Pierre and Marie Curie University - Paris 6
51 PUBLICATIONS **982** CITATIONS
SEE PROFILE

New Insights on the Distribution of Interlayer Water in Bi-Hydrated Smectite from X-ray Diffraction Profile Modeling of 00*l* Reflections

Eric Ferrage,*[,†,‡] Bruno Lanson,[†] Natalie Malikova,[‡,§] Alain Plançon,[||] Boris A. Sakharov,[†,⊥] and Victor A. Drits[†,]

Environmental Geochemistry Group, LGIT, Maison des Géosciences, Joseph Fourier University, CNRS, BP53, F-38041 Grenoble Cedex 9, France, ANDRA, Parc de la Croix Blanche, 1-7 rue Jean Monnet, F-92298 Châtenay-Malabry Cedex, France, Laboratory Liquides Ioniques & Interfaces Chargées, Paris 06 University, Case Courrier 51, 4 Pl. Jussieu, F-75252 Paris, France, Crystallography Laboratory, ISTO, University of Orléans, CNRS, F-45067 Orléans Cedex 2, France, and Geological Institute, Russian Academy of Sciences, 7 Pyzhevsky Street, 109017 Moscow, Russia

Received November 15, 2004. Revised Manuscript Received April 25, 2005

The interlayer configuration proposed by Moore and Reynolds (*X-ray Diffraction and the Identification and Analysis of Clay Minerals*; Oxford University Press: New York, 1997) and commonly used to reproduce the 00*l* reflections of bi-hydrated smectite is shown to be inconsistent with experimental X-ray diffraction data. The alternative configuration of interlayer species with cations located in the mid-plane of the interlayer and one sheet of H_2O molecules on each side of this plane is also shown to imperfectly describe the actual structure of bi-hydrated smectites. Specifically, the thermal fluctuation of atomic positions (Debye−Waller factor) used to describe the positional disorder of interlayer H_2O molecules has to be increased to unrealistic values to satisfactorily reproduce experimental X-ray diffraction data when using this model. A new configuration is thus proposed for the interlayer structure of bi-hydrated smectite. Cations are located in the mid-plane of the interlayer, whereas H_2O molecules are scattered about two main positions according to Gaussian-shaped distributions. This configuration allows reproduction of all 00*l* reflections with a high precision, with only one new variable parameter (width of the Gaussian function). The proposed configuration is consistent with those derived from Monte Carlo calculations and allows matching more closely the amount of interlayer water that can be determined independently from water vapor adsorption/desorption isotherm experiments. In addition, the proposed configuration of interlayer species appears valid for both dioctahedral and trioctahedral smectites exhibiting octahedral and tetrahedral substitutions, thus not allowing differentiation of these expandable 2:1 phyllosilicates from their respective interlayer configurations.

Introduction

Smectite is a 2:1 phyllosilicate with a layer structure consisting of an octahedral sheet sandwiched between two siliceous tetrahedral sheets. Isomorphic substitutions in either tetrahedral or octahedral sites induce a permanent negative layer charge, which is compensated for by the presence of hydrated cations in the interlayer. The observation of 00*l* basal reflections on X-ray diffraction (XRD) patterns has shown that with increasing relative humidity smectite expands stepwise, with the different steps corresponding to the intercalation of 0, 1, 2, or 3 sheets of H_2O molecules in the interlayer.[1−6] From these pioneering studies, it is now commonly accepted that the expandability of 2:1 phyllosilicates is controlled by factors such as the nature of interlayer cations, and the layer charge and its location (octahedral vs tetrahedral). These general observations have led to different models in which crystalline swelling is controlled by the balance between the repulsive forces between neighboring 2:1 layers and the attractive forces between hydrated interlayer cations and the negatively charged surface of siloxane sheets.[6−11]

The development of XRD modeling techniques allowed investigation of structures in which different hydration states coexist, thus improving these early observations.[12−17] Ferrage

* To whom correspondence should be addressed. E-mail: e.ferrage@nhm.ac.uk.
† Joseph Fourier University, CNRS.
‡ ANDRA.
§ Laboratory Liquides Ioniques & Interfaces Chargées, Paris 06 University.
|| University of Orléans, CNRS.
⊥ Russian Academy of Sciences.

(1) Moore, D. M.; Reynolds, R. C., Jr. *X-ray Diffraction and the Identification and Analysis of Clay Minerals*; Oxford University Press: Oxford and New York, 1997.
(2) Nagelschmidt, G. *Z. Kristallogr.* **1936**, *93*, 481−487.
(3) Bradley, W. F.; Grim, R. E.; Clark, G. F. *Z. Kristallogr.* **1937**, *97*, 260−270.
(4) Mooney, R. W.; Keenan, A. G.; Wood, L. A. *J. Am. Chem. Soc.* **1952**, *74*, 1371−1374.
(5) Walker, G. F. *Clays Clay Miner.* **1956**, *4*, 101−115.
(6) Norrish, K. *Discuss. Faraday Soc.* **1954**, *18*, 120−133.
(7) Van Olphen, H. *J. Colloid Sci.* **1965**, *20*, 822−837.
(8) Kittrick, J. A. *Soil Sci. Soc. Am. J.* **1969**, *33*, 217−222.
(9) Kittrick, J. A. *Soil Sci. Soc. Am. J.* **1969**, *33*, 222−225.
(10) Laird, D. A. *Clays Clay Miner.* **1996**, *44*, 553−559.
(11) Laird, D. A. *Clays Clay Miner.* **1999**, *47*, 630−636.
(12) Ben Brahim, J.; Besson, G.; Tchoubar, C. In *5th Meeting of the European Clay Groups*: Prague, 1983; pp 65−75.
(13) Ben Brahim, J.; Besson, G.; Tchoubar, C. *J. Appl. Crystallogr.* **1984**, *17*, 179−188.
(14) Bérend, I.; Cases, J. M.; François, M.; Uriot, J. P.; Michot, L. J.; Masion, A.; Thomas, F. *Clays Clay Miner.* **1995**, *43*, 324−336.
(15) Cases, J. M.; Bérend, I.; Besson, G.; François, M.; Uriot, J. P.; Thomas, F.; Poirier, J. P. *Langmuir* **1992**, *8*, 2730−2739.

10.1021/cm047995v CCC: $30.25
Published on Web 06/01/2005

et al. used such a modeling approach to characterize the hydration of several montmorillonite and beidellite samples and observed that the nature of the interlayer cation, and in particular its affinity for water, influences the layer thickness of bi-hydrated and monohydrated layers.[18,19] They also confirmed that the relative proportions of the different layer types, which correspond to the different hydration states, depend on both the amount and the location of smectite layer charge. In addition, these authors showed that XRD peak profiles and positions can be satisfactorily reproduced, especially over the low-angle region (~5−12° 2θ Cu Kα), only if hydration heterogeneity is taken into account. They were thus able to refine the structure of smectite and in particular to investigate atomic positions of interlayer species. In particular, they showed that the atomic positions reported by Moore and Reynolds for H_2O molecules in bi-hydrated layers induce a dramatic misfit over the medium- to high-angle region (12−50° 2θ Cu Kα) by strongly modifying the intensity ratio between the different 00*l* reflections.[1,18]

The present article thus aims at further refining the structure of interlayer H_2O in bi-hydrated smectites from the fit of experimental XRD patterns. The proposed structure is compared with the positional distribution commonly derived from Monte Carlo simulations, whereas the adjusted amounts of interlayer water are compared with those determined experimentally from water vapor adsorption−desorption experiments.

Background

Smectite Hydration Heterogeneity as seen by XRD Profile Modeling. In agreement with the stepwise evolution of the d_{001} basal spacing on XRD patterns, the hydration state of smectite has been described using three layer types exhibiting different layer thicknesses corresponding to the common hydration states reported for smectite in nonsaturated conditions. Dehydrated layers (0W, layer thickness ~9.6−10.1 Å), monohydrated layers (1W, layer thickness ~12.3−12.7 Å), and bi-hydrated layers (2W, layer thickness ~15.1−15.8 Å) have thus been defined. In the first two layer types, interlayer cations are located in the mid-plane of the interlayer, together with H_2O molecules for 1W layers. For 2W layers, interlayer cations are also commonly assumed to be located in the mid-plane of the interlayer.[1] In addition, it is usually assumed that two planes of H_2O molecules, each bearing 0.69 H_2O per $O_{20}(OH)_4$, are located at 0.35 and 1.06 Å from the cation along the *c** axis (Debye−Waller parameter B_{wat} ~2 Å^2 for these two planes), whereas a third denser plane (1.20 H_2O per $O_{20}(OH)_4$) is located further from the central interlayer cation at 1.20 Å along the *c** axis (B_{wat} = 11 Å^2).[1] The pattern calculated for the Ca-saturated reference SWy-1 montmorillonite (Ca−SWy-1) assuming a homogeneous 2W hydration state and the above configuration for interlayer species is compared in Figure 1a to the experimental pattern recorded at 80% RH. With these usual hypotheses, the calculated pattern fits most of the experimental pattern features but significant discrepancies can be observed over the medium- to high-angle region despite the low intensity diffracted. In particular, the position of the 005 reflection and the low-angle "tail" of the 002 reflection are not well reproduced (Figure 1a). Ferrage et al. challenged

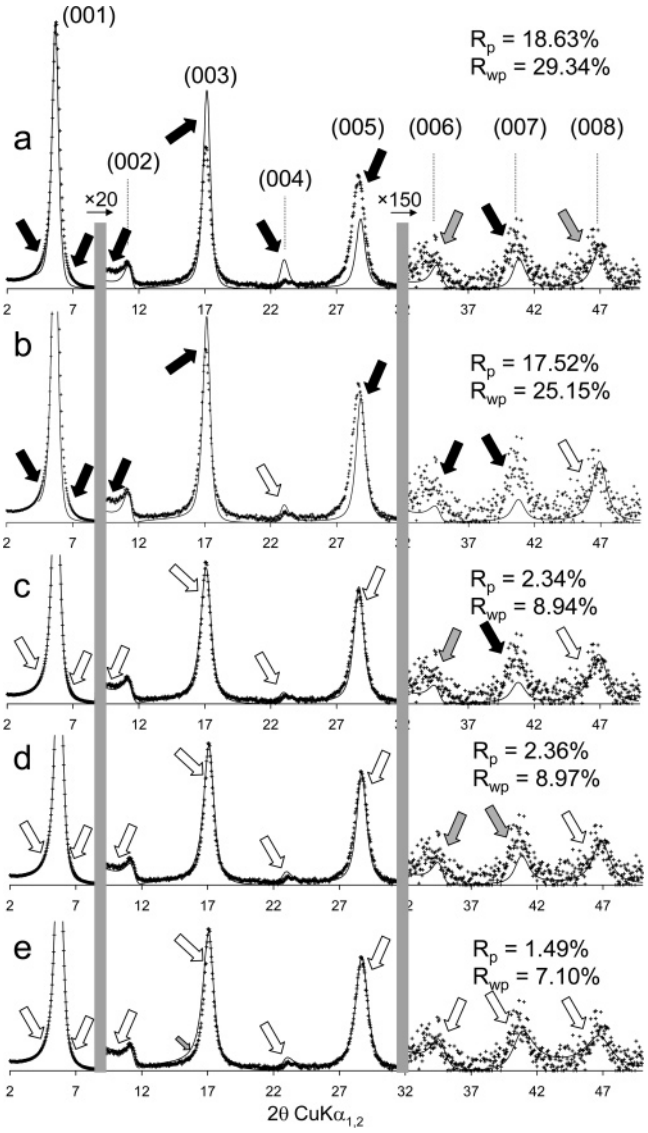

Figure 1. Comparison between experimental and calculated XRD patterns for the Ca-saturated SWy-1 montmorillonite sample recorded at 80% RH. Structural parameters used for the calculations are listed in Tables 1, 2, and 3. Experimental data are shown as crosses whereas calculated profiles are shown as solid lines. Solid arrows indicate a significant misfit between experimental and calculated patterns, whereas gray and open arrows indicate poor and good fits, respectively. 00*l* reflections are indexed in parentheses. (a) Calculation for a periodic bi-hydrated structure (layer thickness of 2W layers = 15.48 Å) assuming the usual configuration of H_2O molecules (ref 1). (b) Calculation for a periodic bi-hydrated structure (layer thickness of 2W layers 15.48 Å) assuming a 2WS configuration (see text for details) with B_{wat} = 2 Å^2 for H_2O molecules (ref 18). (c) Calculation performed accounting for hydration heterogeneities and assuming a 2WS configuration with B_{wat} = 2 Å^2 for H_2O molecules (ref 18). Hydration heterogeneity was described by assuming the coexistence of a major MLS containing 2W and 1W layers (95:5 ratio) and of a second structure containing the three layer types (2W/1W/0W = 85:13:2) in a 61:39 ratio (Table 2). (d) Calculation performed accounting for hydration heterogeneities and assuming a 2WS configuration with B_{wat} = 11 Å^2 for H_2O molecules. (e) Calculation performed accounting for hydration heterogeneities and assuming a 2WG configuration (see text for details).

(16) Cases, J. M.; Bérend, I.; François, M.; Uriot, J. P.; Michot, L. J.; Thomas, F. *Clays Clay Miner.* **1997**, *45*, 8−22.
(17) Cuadros, J. *Am. J. Sci.* **1997**, *297*, 829−841.
(18) Ferrage, E.; Lanson, B.; Sakharov, B. A.; Drits, V. A. *Am. Mineral.* **2005**, in press (MS 1776R).
(19) Ferrage, E.; Lanson, B.; Sakharov, B. A.; Geoffroy, N.; Jacquot, E.; Drits, V. A. *Am. Mineral.* **2005**, in preparation.

this usual configuration of interlayer species, and proposed an alternative configuration that includes a unique plane of H_2O molecules located at 1.20 Å, along the c^* axis, on either side of the central interlayer cation (2WS configuration).[18] The use of this 2WS configuration helps to reduce the discrepancies observed for the 003−005 reflections. In particular, this configuration allows decreasing the relative intensity of the 003 and 004 reflections, whereas the intensity of the 005 one is increased (Figure 1b). However, in the high-angle region the intensity ratio between the 007 and 008 reflections measured on the calculated pattern is inconsistent with that determined experimentally, although the intensity of the 008 reflection is correctly reproduced.

Ferrage et al. also demonstrated that the common hypothesis of a homogeneous hydration state for smectite is not consistent with the likely existence in smectite of structural heterogeneities affecting the layer charge distribution (from one interlayer to the other or within a given interlayer) and/or location (octahedral vs tetrahedral).[18] In turn these heterogeneities lead to the coexistence of different layer types in a single structure. Such hydration heterogeneity has been evidenced from the profile modeling of XRD patterns recorded on hydrated smectites.[12−17] Ferrage et al. have shown that this heterogeneity is systematically observed whatever the interlayer cation, the relative humidity (RH), and the amount and location of the layer charge deficit.[18,19] It is thus essential to account for the hydration heterogeneity to satisfactorily reproduce the experimental positions and profiles of reflections.

Ferrage et al. have shown indeed that accounting for smectite hydration heterogeneity allows better fitting of the profiles of all experimental 00*l* reflections.[18,19] In particular, heterogeneous samples were modeled by combining the contributions of several structures, each containing either one (periodic structure) or different layer types (mixed-layer structure, MLS) randomly interstratified ($R = 0$).[18−20] These different contributions should be seen as a simplified way to describe the actual hydration heterogeneity of the sample under investigation, with the different layer types not being distributed at random in the different crystallites. However, the coexistence of these contributions does not imply the actual presence of populations of particles in the sample, as their relative proportions may vary as a function of RH for example.[18] To account for the heterogeneous distribution of the different layer types within smectite crystallites, layers exhibiting the same hydration state that are present in the different MLSs must have identical properties as they may be accounted for in one or the other structure depending on the RH. In particular, for a given XRD pattern, each layer type must possess a constant crystal chemistry in the different MLSs. It was possible to reproduce the profile of all experimental 00*l* reflections of the experimental XRD pattern recorded on Ca−SWy-1 at 80% RH by considering two MLSs (Figure 1c) and the 2WS configuration for interlayer water.[18] Specifically, the position of the 005 reflection, the low-angle shoulder of the 002 reflection, and the "tails" of the 001 reflection are satisfactorily reproduced by taking hydration heterogeneity into account. Accounting for hydration heterogeneity also helps to reproduce the relative intensity of higher-angle reflections (002, 003, 004, and 005, for example) but significant discrepancies that could result from an incorrect structure model for interlayer water are still visible for high-angle reflections (Figure 1c). Specifically, the 006, 007, and 008 reflections are not satisfactorily reproduced, as, for example, the intensity ratio between the 007 and 008 reflections measured on experimental and calculated patterns are inconsistent. These discrepancies are reduced by increasing the Debye−Waller factor of H_2O molecules (B_{wat}) from 2 to 11 Å^2 for this 2WS configuration of interlayer H_2O molecules (Figure 1d).[18] However, such high values of the Debye−Waller factor are not sufficient to conceal the disagreement for the intensity ratio between 007 and 008 reflections, and thermal atomic fluctuations most likely do not adequately describe the positional distribution of H_2O molecules in 2W smectite layers, and additional hypotheses have to be sought.

Interlayer Configuration of 2W Smectite Layers as seen by Monte Carlo Simulations. In the above calculations, H_2O molecules are distributed in discrete planes, and the positional distribution of H_2O molecules results only from their thermal motion. However, this simplified description of the smectite interlayer structure does not allow fitting of the experimental XRD data (Figure 1c and d), most likely because the description of H_2O molecule positional disorder is incomplete. A more complete (and perhaps realistic) description of the interlayer structure may be obtained from Monte Carlo (MC) simulations which allow taking into account all interactions among interlayer species, as well as those between these species and the 2:1 layer.[21] It is in particular possible to account for the hydration variability of interlayer cation which can form either inner-sphere or outer-sphere complexes with the 2:1 layer surface, leading to the existence or to the lack, respectively, of direct interactions with O atoms from the layer surface. In the latter case, these interactions are screened by H_2O molecules from the cation hydration sphere. It has been shown that, as compared to other monovalent cations, K^+ cations tend to form inner-sphere complexes in montmorillonite interlayers and that these cations remain partially bound to the 2:1 clay surface even in the 2W state.[22,23] In contrast, Li^+ and Na^+ cations in 2W smectites are located in the mid-plane of the interlayer.[23−26] The location of the layer charge deficit has also been shown to influence the hydration of interlayer Na^+ cations, with the formation of inner-sphere complexes being favored by tetrahedral substitutions.[26] On the other hand, a majority of interlayer Na^+ cations are located in the mid-plane of the interlayer for octahedrally substituted 2W smectites.[23,24] A

(20) Ferrage, E.; Tournassat, C.; Rinnert, E.; Lanson, B. *Geochim. Cosmochim. Acta* **2005**, *69*, 2797−2812.

(21) Skipper, N. T.; Chang, F. R. C.; Sposito, G. *Clays Clay Miner.* **1995**, *43*, 285−293.

(22) Chang, F. R. C.; Skipper, N. T.; Sposito, G. *Langmuir* **1998**, *14*, 1201−1207.

(23) Boek, E. S.; Coveney, P. V.; Skipper, N. T. *J. Am. Chem. Soc.* **1995**, *117*, 12608−12617.

(24) Chang, F. R. C.; Skipper, N. T.; Sposito, G. *Langmuir* **1995**, *11*, 2734−2741.

(25) Chang, F. R. C.; Skipper, N. T.; Sposito, G. *Langmuir* **1997**, *13*, 2074−2082.

(26) Skipper, N. T.; Sposito, G.; Chang, F. R. C. *Clays Clay Miner.* **1995**, *43*, 294−303.

similar influence of the charge location was reported for K- and Li-saturated 2W smectites.[22,25] In contrast, whatever the charge location, Mg^{2+} cations are systematically octahedrally coordinated in 2W smectites and located in the mid-plane of the interlayer.[27,28] In any case, MC simulations most often indicate that H_2O molecules do not form a discrete plane but rather show that they are distributed about a "most probable" position. In addition, the mixed charge location common in smectite layers, and more especially in those of natural samples, can lead to the coexistence in a single smectite interlayer of different complexes, thus broadening the water distribution profile by perturbing the hydrogen bond network and the orientation of the water dipole.[29] Even though MC simulations do not commonly account for smectite hydration heterogeneity, which is best revealed by XRD analysis, such a description of H_2O molecules positional disorder could be the missing link toward a better structure determination of H_2O configuration in 2W smectite layers.

Materials and Methods

Experimental. Samples investigated in the present work include two reference low-charge montmorillonites (SWy-1 and SWy-2) available from the Source Clays Repository (http://www.clays.org/sourceclays/SourceClays.html) and two synthetic saponite samples. The latter samples were selected because of their contrasting layer charges (0.8 and 1.4 per $O_{20}(OH)_4$).[30,31] The size fractionation of all samples, and their homoionic saturation were performed as described by Ferrage et al.[18] For all samples, oriented slides were prepared by drying at room temperature a clay slurry pipetted onto a glass slide. XRD patterns were then recorded using a Bruker D5000 diffractometer equipped with a Kevex Si(Li) solid-state detector, and an Ansyco rh-plus 2250 humidity control device coupled to an Anton Paar TTK450 chamber. Usual scanning parameters were 0.04° 2θ as step size and 6 s as counting time per step over the 2−50° 2θ Cu Kα angular range. The divergence slit, the two Soller slits, and the antiscatter and resolution slits were 0.5°, 2.3°, 2.3°, 0.5°, and 0.06°, respectively. Data collection conditions (60 and 80% RH for Sr-saturated samples, 40 and 80% RH for Ca-saturated samples, and 80 or 90% RH for Na-saturated samples) were selected because of the high amount of 2W layers (>90%) present in these conditions.[18]

Simulation of X-ray Diffraction Data. The algorithms developed initially by Drits and co-workers were used to fit experimental XRD profiles over the 2−50° 2θ Cu Kα range using a trial-and-error approach.[32−34] Instrumental and experimental factors such as horizontal and vertical beam divergences, goniometer radius, and length and thickness of the oriented slides were measured and introduced without further adjustment. The mass absorption coefficient (μ*) was set to 45 cm^2g^{-1}, as recommended by Moore and Reynolds,[1] whereas the parameter characterizing the preferred orientation of the particles in the sample (σ*) was considered as a variable parameter. Additional variable parameters included the coherent scattering domain size (CSDS) along the *c** axis which was characterized by a maximum CSDS value, set to 45 layers, and by a variable mean CSDS value (N).[35] In addition, because of the weak bonds between adjacent smectite layers, layer thickness was allowed to deviate from the average d_{001} value. This cumulative deviation from periodicity, which is described as a "disorder of the second type",[36,37] is accounted for by introducing a variance parameter σ_z.[18] z-coordinates of all atoms building up the 2:1 layer framework, as well as those present in the interlayer of 0W and 1W layers, were set as proposed by Moore and Reynolds.[1] The interlayer structure of 2W layers has been refined to account for all features of experimental XRD patterns recorded on 2W-dominated samples. In particular, a double Gaussian distribution of H_2O molecules along the *c** axis (2WG) was assumed. This 2WG model accounts for both the presence of a unique plane of H_2O molecules on either side of the mid-plane (Figure 1c and d) and the positional distribution of H_2O molecules derived from MC simulations. The 2WG distributions considered in the present study are symmetrical relative to the interlayer mid-plane. They are characterized by the distance (Δd) between this mid-plane, where interlayer cations are supposed to be located, and the position of the maximum density of the Gaussian distribution. In addition, the total amount of interlayer H_2O molecules was refined together with the full width at half-maximum intensity (fwhm) parameter of the Gaussian distribution. In the resulting structure model, H_2O molecules were introduced using a 0.05-Å step along the *c** axis, with a B_{wat} factor equal to zero, as thermal motion is taken into account in MC calculations.

Two parameters were used to assess the overall goodness of fit. The unweighted R_p parameter was considered because this parameter is mainly influenced by the most intense diffraction maxima such as the 001 reflection which contains essential information on the proportions of the different layer types and on their respective layer thickness values. The R_{wp} parameter was also used to better account for the overall fit quality, especially in the high-angle regions.[38] Accessory quartz reflections were omitted for the calculation of these parameters. On their low-angle side, calculated XRD patterns are limited to ~5° 2θ Cu Kα because significant discrepancies, possibly resulting from an incorrect description of crystalline defects not challenging the results described in the present study,[18] are observed over the low-angle region.[39]

Monte Carlo Simulations. Monte Carlo simulations in the NVT ensemble were used to obtain a detailed spatial distribution of the different species within smectite interlayers. The model montmorillonite-type smectite used in the simulations has a $Na_{0.75}(Si_8)(Al_{3.25}Mg_{0.75})O_{20}(OH)_4$ structural formula and exhibits substitutions only in the octahedral sheet. The simulation box includes two 2:1 layers, each consisting of 8 unit cells (total area 20.72 Å × 17.94 Å, thickness of the 2:1 layer 6.54 Å). The total negative charge of the 2:1 layers was thus compensated for by 6 Na^+ cations in the interlayer. The interlayer shift between adjacent 2:1 layers was set

(27) Skipper, N. T.; Refson, K.; McConnell, J. D. C. *J. Chem. Phys.* **1991**, *94*, 7434−7445.
(28) Greathouse, J.; Refson, K.; Sposito, G. *J. Am. Chem. Soc.* **2000**, *122*, 11459−11464.
(29) Sposito, G.; Skipper, N. T.; Sutton, R.; Park, S. H.; Soper, A. K.; Greathouse, J. A. *Proc. Nat. Acad. Sci. U.S.A.* **1999**, *96*, 3358−3364.
(30) Michot, L. J.; Villiéras, F. *Clay Miner.* **2002**, *37*, 39−57.
(31) Pelletier, M.; Michot, L. J.; Humbert, B.; Barres, O.; d'espinose de la Callerie, J. B.; Robert, J. L. *Am. Mineral.* **2003**, *88*, 1801−1808.
(32) Drits, V. A.; Sakharov, B. A. *X-ray Structure Analysis of Mixed-Layer Minerals*; Nauka: Moscow, 1976.
(33) Drits, V. A.; Lindgreen, H.; Sakharov, B. A.; Salyn, A. S. *Clay Miner.* **1997**, *33*, 351−371.
(34) Sakharov, B. A.; Lindgreen, H.; Salyn, A.; Drits, V. A. *Clays Clay Miner.* **1999**, *47*, 555−566.
(35) Drits, V. A.; Srodon, J.; Eberl, D. D. *Clays Clay Miner.* **1997**, *45*, 461−475.
(36) Guinier, A. *Théorie et Technique de la Radiocristallographie*; Dunod: Paris, 1964.
(37) Drits, V. A.; Tchoubar, C. *X-ray Diffraction by Disordered Lamellar Structures: Theory and Applications to Microdivided Silicates and Carbons*; Springer-Verlag: Berlin, 1990.
(38) Howard, S. A.; Preston, K. D. In *Modern Powder Diffraction*; Bish, D. L., Post, J. E., Eds.; Mineralogical Society of America: Washington, DC, 1989; Reviews in Mineralogy Vol. 20, pp 217−275.
(39) Plançon, A. *Am. Mineral.* **2002**, *87*, 1672−1677.

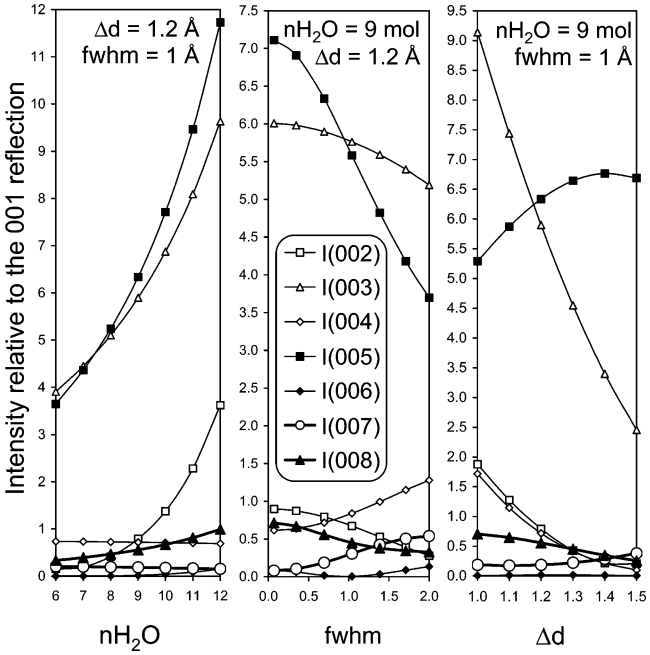

Figure 2. Relative intensities of 00*l* reflections, after normalization to the 001 reflection, as a function of structural parameters specific to the 2WG configuration (see text for details). The total amount of H_2O molecules (nH_2O) is given per $O_{20}(OH)_4$, whereas the full width at half-maximum intensity (fwhm) of the distribution and the distance, in projection along the *c** axis, from its maximum to the interlayer mid-plane (Δd) are given in Å.

to different arbitrary values for the two interlayers considered and not allowed to vary during the calculation. For the typical layer thickness value (15.52 Å) determined for Na-montmorillonite by XRD profile modeling, the water content was estimated from the results of previous MC simulations performed with the NPT ensemble. The series of such simulations allows the determination of layer thickness as a function of water content, at constant pressure and temperature,[40] and the water content was found to be 9.5 H_2O molecules per $O_{20}(OH)_4$. The resulting distributions of H_2O molecules within 2W smectite interlayers were collected over 5 million MC steps, normalized, and made symmetric with respect to the mid-plane of the interlayer. The 2:1 layers were considered as rigid, and modeled with the rigid SPC/E model (O−H bond 1.0 Å, angle H−O−H 109.47°, charges −0.848 e^- and +0.424 e^- for oxygen and hydrogen atoms, respectively). Applied interaction potentials were the Lennard−Jones 6−12 and Coulombic potentials. Each atom in the simulation cell was thus characterized by two van der Waals parameters and by its charge. Additional details on the MC simulations can be found elsewhere.[25,41−43] Density profiles determined from MC calculations for interlayer sodium and H_2O molecules were introduced in the XRD profile calculation using a 0.075-Å step.

Results

Influence of the Gaussian Distribution Profile on the Relative Intensity of 00*l* Reflections. Figure 2 illustrates the influence of the different parameters used to describe the Gaussian distribution of H_2O molecules, that is the total amount of H_2O molecules (nH_2O), Δd, and fwhm, on the relative intensity of 00*l* reflections. Calculations were performed assuming a periodic Ca−SWy-1 2W structure (layer thickness = 15.2 Å), and calculated intensities were systematically normalized to that of the 001 reflection. By increasing the total amount of H_2O molecules the intensity of the 002, 003, 005 reflections greatly increases, that of the 008 reflection also increases but to a lower extent, whereas 004, 006, and 007 reflections are essentially unaffected (Figure 2). As its influence on 007 and 008 reflection intensity is limited, the nH_2O parameter will not significantly affect the intensity ratio between these two reflections, which is a common and critical discrepancy between experimental and calculated profiles (Figure 1a−d). In contrast, the 008:007 intensity ratio is strongly affected by the fwhm of the Gaussian distribution, with this ratio being minimum for a Dirac distribution and increasing with the fwhm of the distribution. The 007 reflection is actually more intense than the 008 one for fwhm values larger than ∼1.3 Å (Figure 2). In addition this parameter may be strongly constrained from its major influence on the intensity ratio between two intense reflections (003 and 005 reflections) which can be reversed by increasing the width of the Gaussian distribution of H_2O molecules. However, the 003:005 ratio is also affected by the Δd parameter which also affects the 008:007 intensity ratio, with both ratios increasing with increasing Δd values. By increasing either the Δd parameter or the fwhm, the intensity of the 002 reflection is systematically decreased, whereas that of the 004 reflection is increased or decreased, respectively. The intensity calculated for the 006 reflection is low regardless of the values used for these two parameters.

Modeling of XRD Patterns. For all XRD patterns recorded on smectite samples, calculations were performed using three different configurations of H_2O molecules in the interlayers of 2W layers: (i) a 2WS configuration with two planes of H_2O molecules characterized by a B_{wat} factor of 2 $Å^2$ and a Δd parameter of 1.2 Å,[18] (ii) a similar 2WS configuration with a larger Debye−Waller factor (B_{wat} = 11 $Å^2$), and (iii) a configuration with H_2O molecules distributed according to the 2WG configuration. Optimum parameters used to characterize smectite hydration heterogeneity, that is the relative proportions of the different MLSs coexisting in the sample and their compositions (relative proportions of 2W, 1W, and 0W layers), are reported in Table 1 together with the layer thickness values for the different layer types, N, σ^*, σ_z, and the water content in 1W layers. For 2W layers, the water content, the Δd parameter, and the fwhm of the Gaussian distribution are reported in Table 2 for the different configurations of interlayer H_2O molecules.

Ca-Saturated Montmorillonite. For sample Ca−SWy-1 at 80% RH, the calculations performed for 2WS configurations of H_2O molecules (Δd = 1.2 Å) and B_{wat} factors of 2 and 11 $Å^2$ have been described above (Figure 1c and d). The 2WS configuration provides a satisfactory fit to experimental patterns for 00*l* reflections with $l < 6$. However, this model does not allow concealing the discrepancy observed over the high-angle range, and more especially for the 008:007 intensity ratio, even if the Debye−Waller factor of H_2O

(40) Marry, V. Ph.D. Dissertation, Pierre et Marie Curie University, Paris, 2002.
(41) Marry, V.; Turq, P.; Cartailler, T.; Levesque, D. *J. Chem. Phys.* **2002**, *117*, 3454−3463.
(42) Delville, A. *Langmuir* **1992**, *8*, 1796−1805.
(43) Boek, E. S.; Coveney, P. V.; Skipper, N. T. *Langmuir* **1995**, *11*, 4629−4631.

Table 1. Optimum Structural Parameters Used for the Simulation of Experimental XRD Profiles

sample	rel. ab. (%)[a]	2W[b]	1W[b]	0W[b]	layer thickness[c] 2W	1W	0W	nH$_2$O 1W[d]	N[e]	σ^*[f]	σ_z[g]
Ca−SWy-2 (40%RH)[h]	87	100	0	0	15.18	12.60	10.00	3.2	8.7	6.5	0.35
	13	60	30	10							
Ca−SWy-1 (80%RH)[i]	61	95	5	0	15.51	12.85	10.00	3.3	6.0	6.5	0.27
	39	85	13	2							
Sr−SWy-1 (60%RH)[i]	82	100	0	0	15.53	12.58	10.00	3.5	7.5	5.5	0.35
	18	75	15	10							
Sr−SWy-1 (80%RH)[i]	84	100	0	0	15.73	12.70	10.00	5.5	7.5	5.5	0.35
	16	75	15	10							
Na−SWy-2 (80%RH)	90	96	2	2	15.52	12.55	9.60	3.2	8.2	11.0	0.25
	10	60	30	10							
Na−Sap$_{0.8}$ (90%RH)	44	100	0	0	15.40	13.20	9.80	5.7	13.0	2.0	0.19
	56	90	5	5							
Na−Sap$_{1.4}$ (90%RH)	91	100	0	0	15.00	12.90	9.80	5.0	12.0	11	0.12
	9	70	20	10							

[a] Relative proportion of the different contributions to the diffracted intensity. [b] Relative proportion of the different layer types in the different contributions to the diffracted intensity. 2W, 1W, and 0W stand for bi-hydrated, monohydrated and de-hydrated smectite layers, respectively. [c] Layer thickness of the different layer types. [d] Number of H_2O molecules in 1W layers (per $O_{20}(OH)_4$). [e] Mean thickness of the coherent scattering domain size along the c* axis (in layers). [f] σ^* parameter characterizing the sample orientation (in deg, ref 1). [g] Standard deviation of the layer thickness parameter (in Å) (ref 18). [h] Data from Ferrage et al (ref 20). [i] Data from Ferrage et al (ref 18).

Table 2. Structural Parameters of the Interlayer Space Determined from XRD Profile Modeling as a Function of the Assumed Water Configuration

sample	2WS, $B_{wat} = 2$[a] nH$_2$O[c]	Δd[d]	2WS, $B_{wat} = 11$[a] nH$_2$O	Δd	2WG[b] nH$_2$O	Δd	fwhm[e]
Ca−SWy-2 (40%RH)	6.2	1.20	6.6	1.30	7.8	1.34	1.4
Ca−SWy-1 (80%RH)	6.6	1.20	6.8	1.32	10.0	1.37	1.7
Sr−SWy-1 (60%RH)	6.0	1.20	6.8	1.32	8.5	1.40	1.2
Sr−SWy-1 (80%RH)	6.0	1.20	7.0	1.41	9.5	1.52	1.5
Na−SWy-2 (80%RH)	7.4	1.20	8.2	1.41	9.5	1.50	1.4
Na−Sap$_{0.8}$ (90%RH)	8.5	1.20	9.3	1.33	10.5	1.39	1.4
Na−Sap$_{1.4}$ (90%RH)	8.4	1.20	9.0	1.33	9.4	1.35	0.8

[a] 2WS corresponds to an interlayer configuration of H_2O molecules distributed as one plane on either side of the interlayer mid-plane. The Debye−Waller temperature factor for water (B_{wat}) is given in Å^2. [b] 2WG corresponds to an interlayer configuration of H_2O molecules distributed according to a Gaussian function on either side of the interlayer mid-plane. [c] The number of H_2O molecules is given per $O_{20}(OH)_4$. In this case, B_{wat}= 0 Å^2. [d] The distance, in projection along the c^* axis, between the interlayer mid-plane and the maximum density of the distribution of H_2O molecules (Δd) is given in Å. [e] The width of the Gaussian distribution of interlayer H_2O molecules (fwhm) is given in Å.

molecules is maximized (B_{wat} = 10−11 Å^2).[44] In this case, the water content and the Δd parameter are increased from 6.6 to 6.8 H_2O per $O_{20}(OH)_4$ and from 1.20 to 1.32 Å, respectively, as compared to the 2WS configuration with B_{wat} = 2 Å^2 (Table 2). A 008:007 intensity ratio consistent with that observed experimentally can be obtained by considering the 2WG configuration for interlayer H_2O molecules. In this case, broad Gaussian distributions were assumed (fwhm = 1.7 Å), and both the water content and the Δd parameter were increased as compared to alternative interlayer configurations (Table 2). This 2WG configuration also allows better fitting of the profile of the 005 reflection, but that of the 003 one is slightly altered as a result of a low-angle tail broadening (Figure 1e).

The combination of two structures, a main periodic one with only 2W layers and a second one containing the three layer types (Table 1), accounts for the hydration heterogeneity of sample Ca−SWy-2 at 40% RH, and leads to the coexistence of 2W, 1W, and 0W layers (95%, 4%, and 1%, respectively).[18] The 2WS configuration allows describing most features of the experimental XRD patterns (R_p = 1.31% and R_{wp} = 8.13%, Figure 3a). However, the 008 reflection is significantly more intense than the 007 one. By increasing the Debye−Waller B_{wat} factor from 2 to 11 Å^2, the 008:007 intensity ratio appears closer to the experimental one, although the two estimates of the fit quality are not affected (Figure 3b). This ratio is best reproduced by assuming a 2WG distribution with a fwhm of 1.4 Å (Figure 3c) although R_p and R_{wp} parameters are almost unaffected. As compared to the 2WS mode the total amount of H_2O molecules in such 2WG configuration is considerably increased from 6.2 (assuming a B_{wat} factor of 2 Å^2) to 7.8 per $O_{20}(OH)_4$ (Table 2).

Sr-Saturated Montmorillonite. At both 60 and 80% RH, the hydration heterogeneity of sample Sr−SWy-1 is minimum as it contains an overwhelming proportion of 2W layers (95, and 96%, respectively; Table 1).[18] As for the Ca-saturated samples, the 2WS configuration for H_2O molecules leads to a satisfactory fit to the experimental XRD patterns, especially for 00l reflections with l < 6, and for the 008 reflection (Figures 4a and 5a). However, significant discrepancies between experimental and calculated patterns are visible for the 002 reflection and the 008:007 intensity ratio. These discrepancies are significantly reduced by increasing the Debye−Waller factor of H_2O molecules from 2 to 11 Å^2, but they do not vanish completely (Figures 4b and 5b). The optimum fit to the experimental XRD patterns was again obtained assuming a 2WG distribution of interlayer H_2O molecules with a large fwhm value (1.2, and 1.5 Å for Sr−SWy-1 samples recorded at 60 and 80% RH, respec-

(44) Lipson, H. In *International Tables for X-ray Crystallography*; Casper, J. S., Lonsdale, K., Eds.; International Union of Crystallography, 1967; Mathematical tables Vol. 2, pp 235−315.

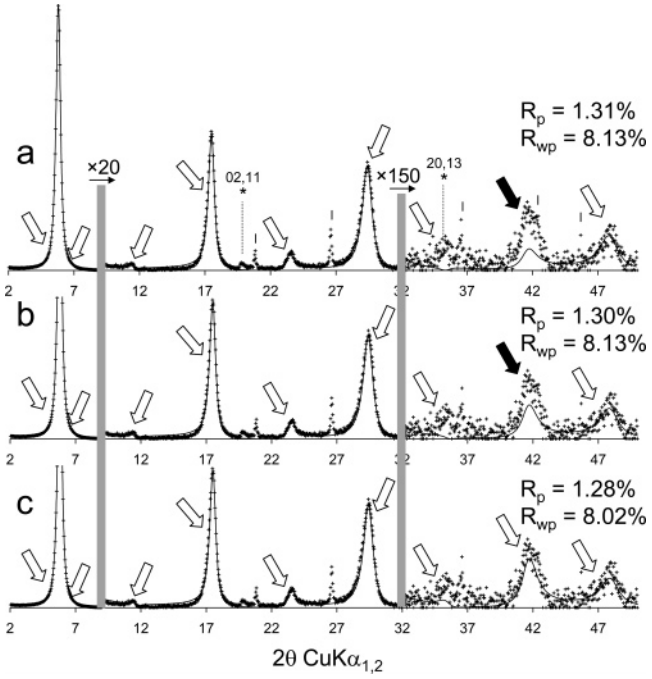

Figure 3. Comparison between experimental and calculated XRD patterns for the Ca-saturated SWy-2 montmorillonite sample recorded at 40% RH. Structural parameters used for the calculations are listed in Tables 1, 2, and 3. Patterns as for Figure 1. (*) indicates hk bands, whereas vertical ticks denote the presence of accessory quartz reflections. (a) Calculation performed assuming a 2WS configuration with B_{wat} = 2 Å^2 for H_2O molecules (ref 18). (b) Calculation performed assuming a 2WS configuration with B_{wat} = 11 Å^2 for H_2O molecules. (c) Calculation performed assuming a 2WG configuration.

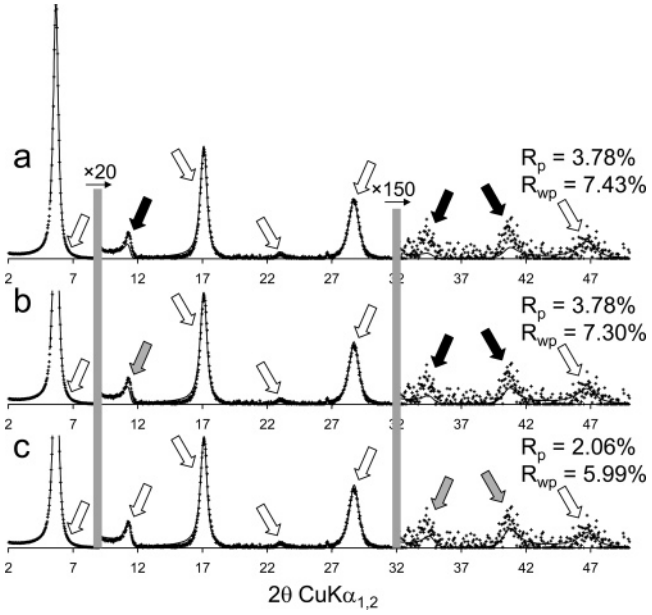

Figure 4. Comparison between experimental and calculated XRD patterns for the Sr-saturated SWy-1 montmorillonite sample recorded at 60% RH. Structural parameters used for the calculations are listed in Tables 1, 2, and 3. Patterns as for Figure 1. (a) Calculation performed assuming a 2WS configuration with B_{wat} = 2 Å^2 for H_2O molecules (ref 18). (b) Calculation performed assuming a 2WS configuration with B_{wat} = 11 Å^2 for H_2O molecules. (c) Calculation performed assuming a 2WG configuration.

tively; Table 2; Figures 4c and 5c). For the two samples, both R_p and R_{wp} are lower for the 2WG configuration of interlayer H_2O molecules than for the 2WS ones.

Na-Saturated Montmorillonite. At 80% RH, the Na−SWy-2 sample exhibits a high proportion (92%) of 2W

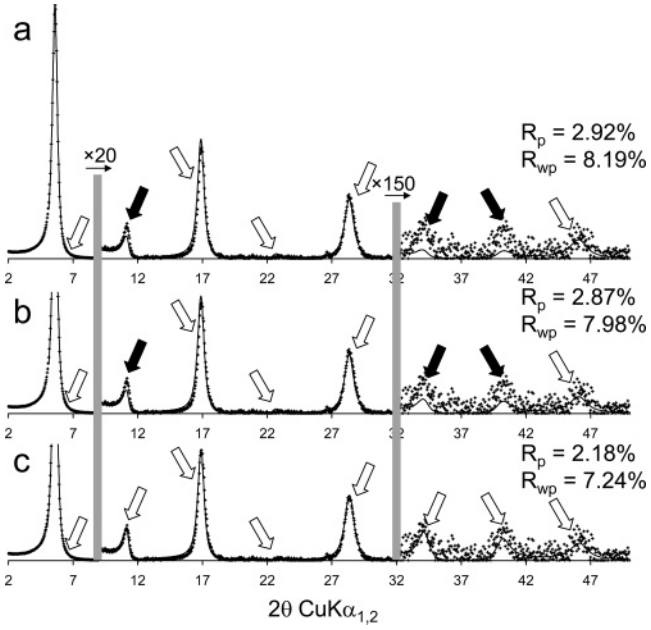

Figure 5. Comparison between experimental and calculated XRD patterns for the Sr-saturated SWy-1 montmorillonite sample recorded at 80% RH. Structural parameters used for the calculations are listed in Tables 1, 2, and 3. Patterns as for Figure 1. (a) Calculation performed assuming a 2WS configuration with B_{wat} = 2 Å^2 for H_2O molecules (ref 18). (b) Calculation performed assuming a 2WS configuration with B_{wat} = 11 Å^2 for H_2O molecules. (c) Calculation performed assuming a 2WG configuration.

layers, whereas minor amounts of 1W and 0W layers (5%, and 3%, respectively) account for the hydration heterogeneity (Table 1). As for the previous sample, the 2WS configuration of H_2O molecules leads to a satisfactory agreement between experimental and calculated data, especially for 00*l* reflections with $l < 6$, and for the 008 reflection (Figure 6a). However, by using a Debye−Waller factor of 2 Å^2 the intensities calculated for the 006 and 007 reflections are too low as compared to the experimental ones. Increasing the B_{wat} factor up to 11 Å^2 significantly reduces these discrepancies, although the 008:007 intensity ratio remains imperfectly reproduced (Figure 6b). The optimum fit to the experimental data for this sample was again obtained assuming a 2WG distribution of H_2O molecules (Figure 6c; R_{wp} = 5.33%, R_p = 2.59%). The Δd and fwhm parameters of this 2WG distribution are 1.50 Å and 1.4 Å, respectively (Table 2). A similar fit to the experimental data (Figure 6d; R_{wp} = 5.34%, R_p = 2.57%) was obtained assuming the distribution of interlayer species shown in Figure 7, while all other parameters were kept constant (Table 1). This distribution was derived from the MC simulations performed using the NVT ensemble. MC calculated distributions exhibit a single peak for the oxygen atoms, and two for the hydrogen atoms, between the interlayer mid-plane and the surface of the 2:1 layer, and are characteristic of the presence of a single plane of H_2O molecules on either side of the cation plane which is located in the center of the interlayer. The distance between the maximum of the oxygen distribution and the maximum of the hydrogen distribution closer to the 2:1 layer is ∼1.0 Å which is the length of the O−H bond in the water molecule. This indicates a preferential orientation of the H_2O molecules in the interlayer, with one of the O−H bonds almost perpendicular to the surface of the 2:1 layer. Similar configurations of H_2O molecules in the interlayer of octa-

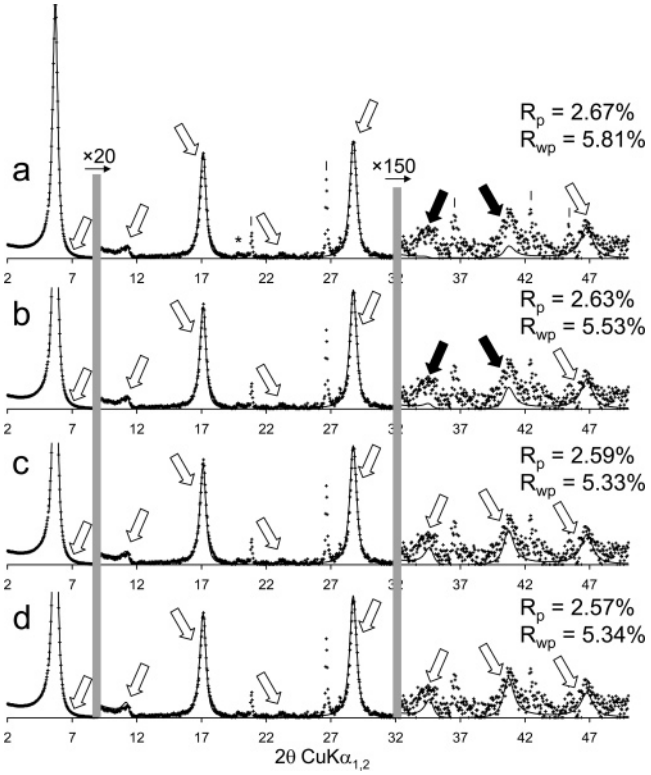

Figure 6. Comparison between experimental and calculated XRD patterns for the Na-saturated SWy-2 montmorillonite sample recorded at 80% RH. Structural parameters used for the calculations are listed in Tables 1, 2, and 3. Patterns as for Figures 1 and 3. (a) Calculation performed assuming a 2WS configuration with $B_{wat} = 2$ Å^2 for H_2O molecules (ref 18). (b) Calculation performed assuming a 2WS configuration with $B_{wat} = 11$ Å^2 for H_2O molecules. (c) Calculation performed assuming a 2WG configuration. (d) Calculation performed assuming the distribution of interlayer species derived from MC simulations using the NVT ensemble and shown in Figure 7.

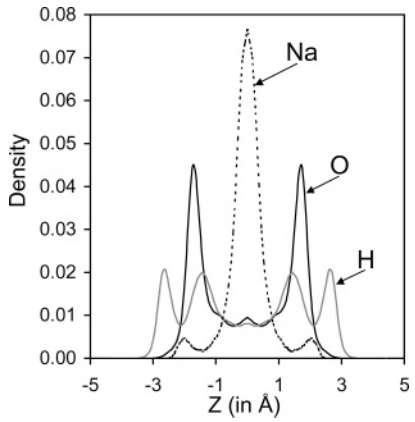

Figure 7. Density profiles of interlayer species along the *c** axis derived from MC simulations performed using the NVT ensemble. *z*-coordinates are given in Å with the origin located in the interlayer mid-plane. Solid, dashed, and gray lines represent O, H, and Na^+ atoms, respectively.

hedrally substituted smectites have been previously reported from IR spectroscopy results[45] and from microscopic simulations.[24] As for all other samples, the amount of interlayer H_2O molecules has to be increased, together with the Δd parameter, as the positional distribution of these species increases (Table 2).

Na-Saturated Synthetic Saponites. At 90% RH, the hydration heterogeneity of both synthetic saponites is minimum

(45) Sposito, G.; Prost, R. *Chem. Rev.* **1982**, *82*, 553−573.

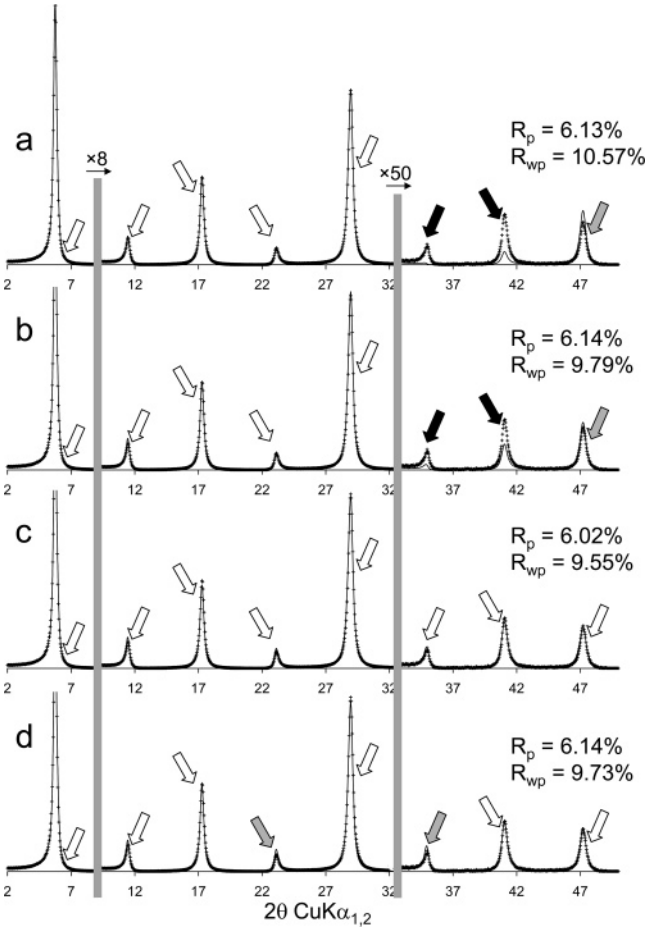

Figure 8. Comparison between experimental and calculated XRD patterns for the Na-saturated $Sap_{0.8}$ saponite sample recorded at 90% RH. Structural parameters used for the calculations are listed in Tables 1, 2, and 3. Patterns as for Figure 1. (a) Calculation performed assuming a 2WS configuration with $B_{wat} = 2$ Å^2 for H_2O molecules (ref 18). (b) Calculation performed assuming a 2WS configuration with $B_{wat} = 11$ Å^2 for H_2O molecules. (c) Calculation performed assuming a 2WG configuration. (d) Calculation performed assuming a 2WS configuration with $B_{wat} = 30$ Å^2 for H_2O molecules, 10.5 H_2O molecules per $O_{20}(OH)_4$) in 2W layers, and Δd =1.38 Å.

as they exhibit an overwhelming proportion of 2W layers (94 and 97% for Na−$Sap_{0.8}$ and Na−$Sap_{1.4}$ samples, respectively; Table 1). As compared to the natural ones, these two synthetic samples present larger CSDS along the *c** axis, as evidenced by the sharpening of the 00*l* reflections (Table 1; Figures 8 and 9). Layer thickness of 2W layers decreases from 15.4 to 15.0 Å as the layer charge increases from 0.8 to 1.4 per $O_{20}(OH)_4$ (samples Na−$Sap_{0.8}$ and Na−$Sap_{1.4}$, respectively; Table 1). For both samples, the 2WS configuration of H_2O molecules with $B_{wat} = 2$ Å^2 allows satisfactory fitting of 00*l* reflections with $l < 6$ (Figures 8a and 9a). Increasing the Debye−Waller factor up to 11 Å^2 leads to a perfect fit to the experimental data for the high-charge sample (Na−$Sap_{1.4}$; Figure 9b), whereas significant discrepancies are still observed between experimental and calculated patterns for the low-charge sample (Na−$Sap_{0.8}$; Figure 8b). For this latter sample, the optimum fit to the experimental data was again obtained assuming a 2WG distribution of H_2O molecules in the smectite interlayer with Δd and fwhm parameters (1.39 and 1.4 Å, respectively) similar to those obtained for natural samples (Figure 8c and Table 2). For the Na−$Sap_{1.4}$ sample, a fit similar to the one obtained with a 2WS distribution of H_2O molecules and a high B_{wat} factor

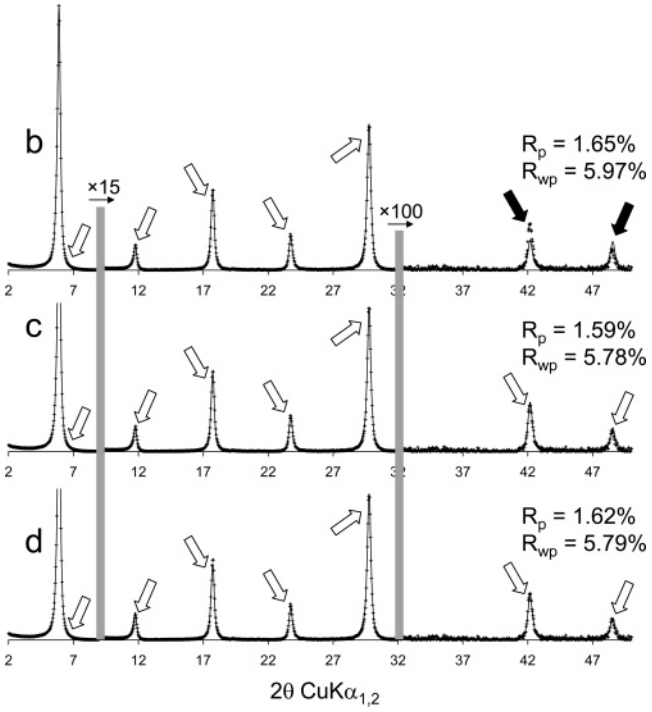

Figure 9. Comparison between experimental and calculated XRD patterns for the Na-saturated $Sap_{1.4}$ saponite sample recorded at 90% RH. Structural parameters used for the calculations are listed in Tables 1, 2, and 3. Patterns as for Figure 1. (a) Calculation performed assuming a 2WS configuration with $B_{wat} = 2$ Å^2 for H_2O molecules (ref 18). (b) Calculation performed assuming a 2WS configuration with $B_{wat} = 11$ Å^2 for H_2O molecules. (c) Calculation performed assuming a 2WG configuration.

was obtained assuming a 2WG distribution of H_2O molecules (Figure 9b and c). However, the fwhm parameter of this distribution is significantly lower (0.8 Å) than those typically obtained for natural samples (1.2−1.7 Å; Table 2).

Discussion

Shortcomings of the Usual Description of H_2O Molecule Positional Disorder in 2W Smectite Interlayers. By accounting for smectite hydration heterogeneity, it is possible to model experimental XRD patterns thus gaining additional insights into the structure of smectite interlayers. It should be noted first that the initial assumption of identical properties for all layers exhibiting the same hydration state and present in the different MLSs was verified for all samples, thus validating the proposed description of smectite hydration heterogeneity. In addition, the configuration of H_2O molecules within 2W smectite layers commonly used for XRD pattern simulations can be discarded as it systematically leads to major discrepancies between experimental and calculated profiles (Figure 10).[18−20] Specifically, the use of this usual configuration systematically leads to poor fits to the experimental XRD patterns for low-angle high-intensity reflections such as 003, 004, and 005 reflections (Figure 10). By contrast, the distribution of H_2O molecules within a single plane on either side of the mid-plane interlayer (2WS configuration) allows both fitting the profiles and reproducing the relative intensities of the 00*l* reflections with $l < 6$ (Figures 1c, 3a, 4a, 5a, 6a, 8a, 9a).[18] When assuming a Debye−Waller B_{wat} factor of 2 Å^2, this model leads to significant discrepancies for high-order 00*l* reflections, which are partly resolved by increasing the positional disorder of H_2O molecules ($B_{wat} = 11$ Å^2; Figures

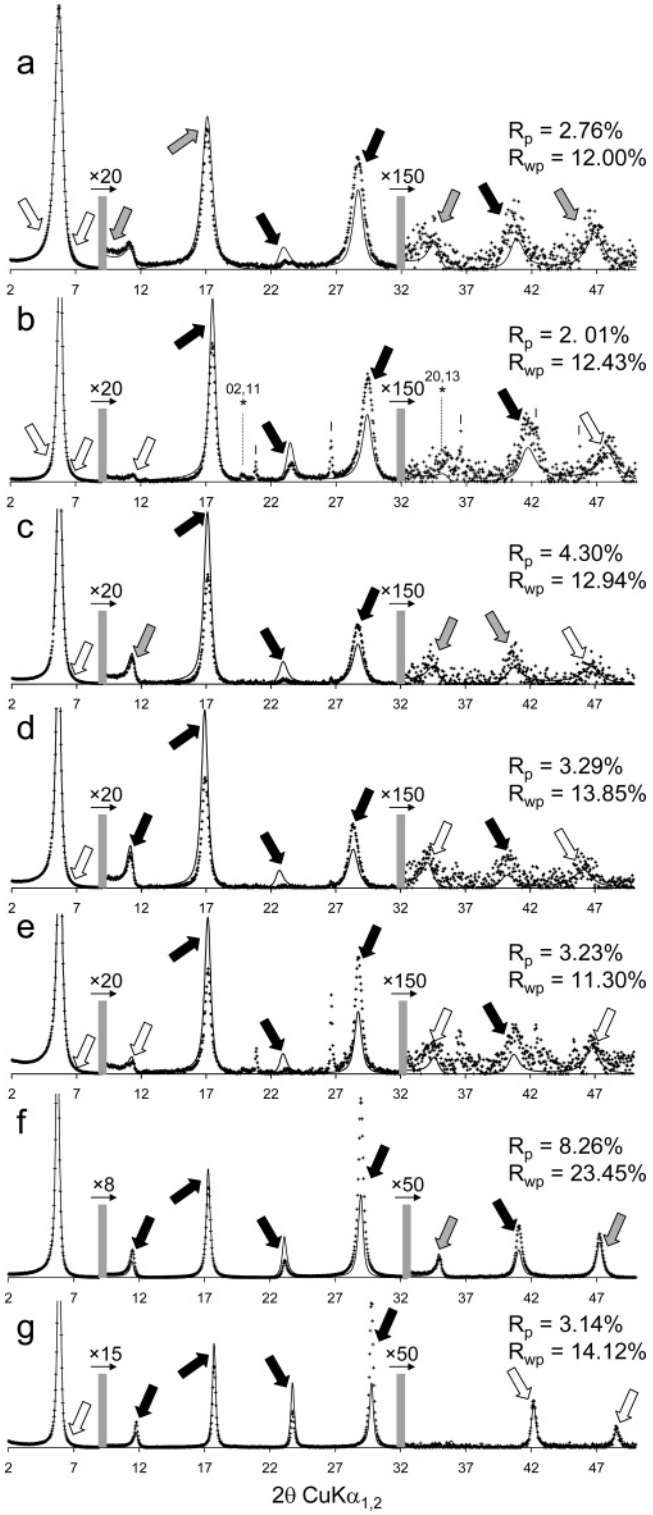

Figure 10. Comparison between experimental XRD patterns and those calculated assuming the usual configuration of H_2O molecules (ref 1). Hydration heterogeneity has been taken into account for all calculations. Structural parameters used for the calculations are listed in Table 1. Patterns as for Figures 1 and 3. (a) Ca-saturated SWy-1 montmorillonite sample recorded at 80% RH. (b) Ca-saturated SWy-2 montmorillonite sample recorded at 40% RH. (c) Sr-saturated SWy-1 montmorillonite sample recorded at 60% RH. (d) Sr-saturated SWy-1 montmorillonite sample recorded at 80% RH. (e) Na-saturated SWy-2 montmorillonite sample recorded at 80% RH. (f) Na-saturated $Sap_{0.8}$ saponite sample recorded at 90% RH. (g) Na-saturated $Sap_{1.4}$ saponite sample recorded at 90% RH.

1d, 3b, 4b, 5b, 6b, 8b, 9b). However, except for sample Na−$Sap_{1.4}$, such an increased B_{wat} factor does not allow satisfactory fitting of the high-order 00*l* reflections, which would

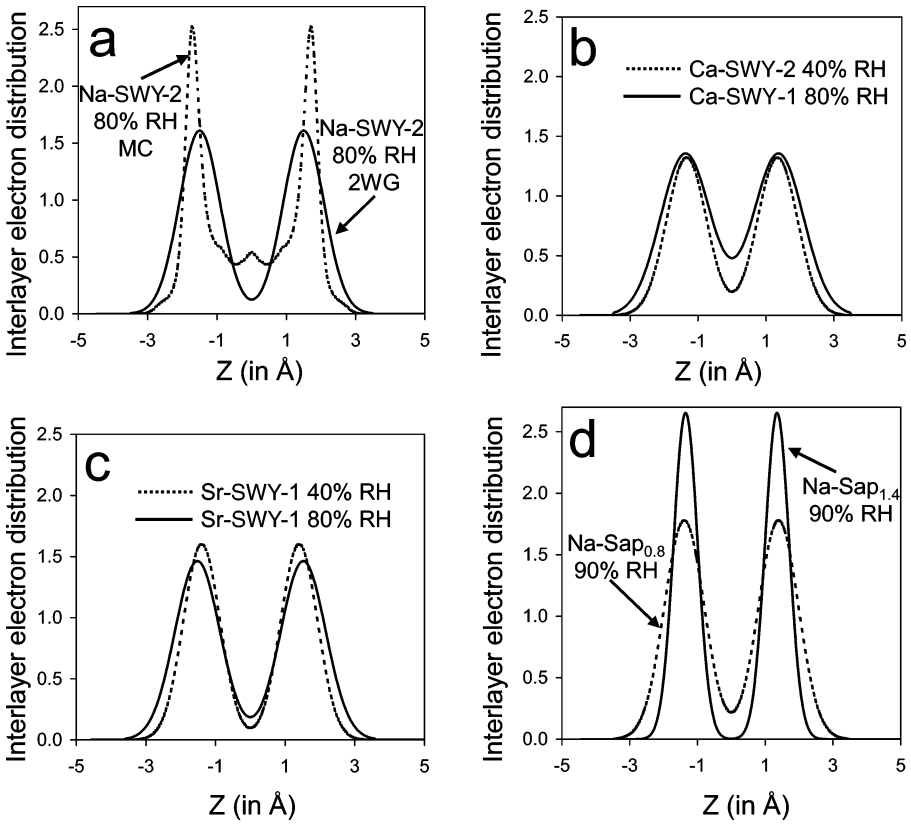

Figure 11. Density profiles along the *c** axis of the electron distribution in the interlayer of bi-hydrated smectite layers. *z*-coordinates are given in Å with the origin located in the interlayer mid-plane. (a) Comparison between the electron distribution derived from the density profiles of interlayer species calculated using the NVT ensemble (Figure 7) and the one determined from XRD profile modeling for the Na−SWy-2 montmorillonite sample (80% RH). (b) Comparison between the electron distributions determined from XRD profile modeling for the two Ca-saturated montmorillonite samples under different RH conditions. (c) Comparison between the electron distributions determined from XRD profile modeling for the two Sr-saturated SWy-1 montmorillonite samples under different RH conditions. (d) Comparison between the electron distributions determined from XRD profile modeling for the two Na-saturated synthetic saponite samples with different amounts of layer charge.

Table 3. Optimum Amounts of H_2O Molecules Determined from XRD Profile Modeling for the Different Configurations of Interlayer Species, and from Water Vapor Adsorption/Desorption Isotherms

sample	type I configuration[a]	2WS B_{wat}= 2[b]	2WS B_{wat}= 11[b]	2WG[c]	ads./des.[d]
Ca−SWy-2 (40%RH)	7.25[e]	8.32	8.58	10.11	8.62/10.17
Ca−SWy-1 (80%RH)	7.06	8.30	8.54	12.36	12.85/13.70
Sr−SWy-1 (60%RH)	7.06	7.60	8.85	10.72	7.87/9.29 (10.70/11.90)
Sr−SWy-1 (80%RH)	7.14	7.69	8.95	12.09	9.83/10.45 (12.80/13.70)
Na−SWy-2 (80%RH)	7.04	9.27	10.24	11.82	10.50/13.10
Na−$Sap_{0.8}$ (90%RH)	7.00	10.62	11.60	13.07	13.39/14.49[f]
Na−$Sap_{1.4}$ (90%RH)	6.96	10.45	11.19	11.62	14.23/17.18[f]

[a] Interlayer configuration of H_2O molecules commonly used for the calculation XRD profiles including 2W layers (ref 1). [b] 2WS corresponds to an interlayer configuration of H_2O molecules distributed as one plane on either side of the interlayer mid-plane. The Debye−Waller temperature factor for water (B_{wat}) is given in Å^2. [c] 2WG corresponds to an interlayer configuration of H_2O molecules distributed according to a Gaussian function on either side of the interlayer mid-plane. In this case, $B_{wat} = 0$ Å^2. [d] Water amounts determined experimentally from water vapor adsorption/desorption isotherms. Data are taken from Cases et al. (ref 16), and from Bérend et al. (ref 14) for divalent and monovalent cations, respectively. [e] The water contents are given in mmol of water per g of clay. [f] Personal communication from Laurent Michot (LEM, Nancy, France).

require unrealistically high B_{wat} factor values. In addition, the contrasting B_{wat} factors adjusted for the two synthetic saponite samples recorded under similar RH and temperature conditions plead for a different origin to the actual positional disorder of H_2O molecules in smectite interlayers.

Distribution of H_2O Molecules According to a Double Gaussian Function. The 2WG model can be considered as an improved version of the 2WS model in which the actual positional disorder of H_2O molecules is better accounted for (Figures 1e, 3c, 4c, 5c, 6c, 8c, 9c). In the 2WG model the interlayer cation is considered to lie in a fixed position located in the interlayer mid-plane and to have a Debye−Waller factor of 2 Å^2. This hypothesis does not imply that the interlayer cations are not distributed as H_2O molecules are, but it was assumed as a first approximation that thermal motion would be sufficient to account for their positional disorder. In addition, the sensitivity to the positional disorder of these cations is much reduced as compared to H_2O molecules, as the former species accounts for a minor part of the overall electronic density in smectite interlayers. For example, at 80% RH Ca^{2+} cations account for only 6% of the interlayer electrons (Table 3).

When comparing the electronic density due to interlayer H_2O molecules deduced from MC calculations with that obtained from XRD profile fitting (Figure 11a), it is possible to note that the overall profiles are globally alike despite significant differences. In particular, the two planes of H_2O molecules on either side of the interlayer mid-plane are much narrower in the MC calculations (fwhm ~0.7 Å as compared to ~1.4 Å for XRD profile fitting) which indicate also a significantly higher electron density in the interlayer mid-plane. The narrower distribution obtained from the MC simulation can be due in part to the fixed interlayer displacement between adjacent layers considered for the calculations, although the influence of interlayer shift and/or layer rotation on the distribution of interlayer species derived from MC simulations is expected to be limited. The simplistic Gaussian functions used to model the distribution of H_2O molecules are both shifted toward the interlayer mid-plane (by about 0.2 Å) and broadened as compared to MC calculations. Both the broadening and the shift of the Gaussian distributions are likely related to the specific profile of the MC distribution, and more especially to the high electron density in the interlayer mid-plane (Figure 7). However, the XRD profiles calculated assuming the two models are almost identical (Figure 6c and d) and plead for a limited sensitivity of calculated XRD patterns to these two parameters if the actual distribution profile is unknown.

Validity of the 2WG Configuration Model. Similar XRD patterns may be calculated with 2WG and 2WS models by increasing the B_{wat} factor in the latter model (Figures 8c and d, and 9b and c). Because of the demonstrated sensitivity of calculated XRD patterns to the distribution of H_2O molecules, this similarity can only result from similar contributions of H_2O molecules to the structure factor in both models. Parameters affecting the structure factor include the scattering power, the position, and the amount of considered species. If the origin of the layer unit is set in the center of the layer octahedron, the contribution of H_2O molecules to the structure factor of 00*l* reflections for a periodic 2W smectite (2WS model) can be expressed as

$$F_{H_2O}(00l) = 2n_{H_2O} f_B\left(\frac{\sin\theta}{\lambda}\right)_{00l} \cos(2\pi lZ) \qquad (1)$$

where $f_B((\sin\theta)/\lambda)_{00l}$ is the scattering power of H_2O molecules taking into account their thermal motion (B_{wat}), n_{H_2O} is the amount of H_2O molecules at $Z = (1/2) - (\Delta d/h)$, h being the layer thickness. Δd is the distance between the interlayer mid-plane and the positions of the H_2O molecules along the c^* axis. With increasing values of l, the contribution of H_2O molecules decreases together with $f_B(00l)$ as a result of the thermal motion of H_2O molecules.

For the 2WG model, the contribution of interlayer H_2O molecules to the structure factor of 00*l* reflections for a periodic 2W smectite can be expressed as

$$F_{H_2O}(00l) = 4f\left(\frac{\sin\theta}{\lambda}\right)_{00l} \cos\left(2\pi l\left(\frac{1}{2} - \frac{\Delta d}{h}\right)\right)\sum_m n_m \cos\left(2\pi lm\frac{\Delta z}{h}\right) \qquad (2)$$

where $f((\sin\theta)/\lambda)_{00l}$ is the scattering power of H_2O molecules ($B_{wat} = 0$), and Δd is the distance along the c^* axis between the interlayer mid-plane and the position of the maximum density of the Gaussian distribution. n_m is the amount of H_2O molecules at a given distance ($m\Delta z$, m being integer) from the maximum density of the Gaussian distribution. The sum $\sum_m n_m$ equals the total number of interlayer H_2O molecules. For a given l value, the positional distribution of H_2O molecules disturbs their coherent scattering and thus decreases their absolute contribution to the structure factor. The decrease becomes more important as the l indice increases. To quantify this decrease, eq 2 can be expressed as

$$F_{H_2O}(00l) = 2n^{eff}_{H_2O} f\left(\frac{\sin\theta}{\lambda}\right)_{00l} \cos\left(2\pi l\left((1/2) - \frac{\Delta d}{h}\right)\right)\sum_m n_m \cos\left(2\pi lm\frac{\Delta Z}{h}\right) \qquad (3)$$

where $n^{eff}_{H_2O} = 2\sum_m n_m \cos(2\pi lm(\Delta Z/h))$ is the effective amount of interlayer H_2O molecules contributing to the structure factor. Eqs 1 and 3 look similar but in the sum determining the $n^{eff}_{H_2O}$ value, the cosine term is lower than 1, and $n^{eff}_{H_2O}$ is thus lower than the total number of H_2O molecules. In addition, the $n^{eff}_{H_2O}$ value decreases with increasing l indices.

Thus, both 2WS and 2WG models are essentially different although in both cases the contribution of interlayer H_2O molecules to the structure factor is strongly decreasing with increasing l indices. In the first case, the thermal motion of these interlayer species is entirely responsible for the decrease, whereas in the latter model the decrease is related to the decreasing effective number of H_2O molecules contributing to coherent diffraction effects. Note that both models may produce similar diffraction effects if appropriate values are used for the parameters describing the positional disorder of interlayer molecules. However, unrealistically large values were obtained for the B_{wat} parameter when fitting $Na-Sap_{0.8}$ ($B_{wat} = 30$ Å^2) as compared to $Na-Sap_{1.4}$ ($B_{wat} = 11$ Å^2) although both XRD patterns were recorded under similar experimental conditions, and the 2WG configuration of H_2O molecules appears as more realistic than the 2WS one. Additional support for the 2WG model arises from the close match between the number of interlayer H_2O molecules determined using the 2WG model and that measured independently from water vapor isotherms.

Water Content in Smectite Interlayer. For a given sample, the total amount of interlayer H_2O molecules can be approximated by weighing the water content hypothesized for each layer type by the relative abundance of this layer type and compared to that obtained from water vapor adsorption−desorption isotherm experiments (Table 3).[18] The water content determined by Ferrage et al. from XRD profile modeling assuming a 2WS model for the distribution of interlayer H_2O molecules was reasonably consistent with that obtained from water vapor adsorption−desorption isotherm experiments.[14,16,18] However, the 2WG configuration provides the best agreement with the water contents determined experimentally from water vapor adsorption−desorption isotherm experiments, with the XRD values lying most often

between the values obtained on either branches of the isotherm (Tables 2 and 3).

fwhm of H_2O Molecule Gaussian Distribution. When using the 2WG model to describe the distribution of H_2O molecules in 2W layers, the fwhm parameter represents the positional disorder of the species, which is characterized by the B_{wat} factor in usual models. One may note that the diffraction effects resulting from the two configurations are similar and lead to a significant decrease of the coherent scattering of H_2O molecules with increasing diffraction angle (see above). However, the B_{wat} factor should be about constant for a given species whereas the fwhm parameter can be structurally interpreted. For example, when increasing the RH, the fwhm of the Gaussian distribution systematically increases for Ca- and Sr-saturated montmorillonites (Table 2, Figure 11b and c) most likely to accommodate the steady addition of H_2O molecules weakly bound to the interlayer cation. On the contrary, with increasing layer charge, Na-saturated saponite samples hold more H_2O molecules for a given RH value in a narrower distribution (Figure 11d and Table 2). A possible origin for such narrowing of H_2O molecule distributions is the increased polarization of these interlayer species resulting from a stronger undersaturation of surface oxygen atoms.

Relative Positions of Interlayer Cations and H_2O Molecules. The distance (Δd) between the interlayer cations, which are located in the interlayer mid-plane, and the maximum density of the interlayer H_2O molecule distribution function was also varied from one model to the other, with the maximum Δd values being obtained with the 2WG configuration of H_2O molecules (Table 2). The Δd values reported in the present study represent only indicative values that could be used for XRD profile modeling but a more complete study should be carried out to determine the key factors that influence this parameter.

Consistency with Reported Interlayer Structures of Expandable 2:1 Phyllosilicates. *Comparison with the Present Data*. Among expandable 2:1 phyllosilicates, vermiculite and smectite are differentiated from their contrasting layer charge, with vermiculite exhibiting a higher layer charge (1.2−1.8 per $O_{20}(OH)_4$) than smectite (0.4−1.2 per $O_{20}(OH)_4$).[46] This difference is usually revealed by the contrasting swelling behavior of the two minerals after magnesium saturation and glycerol solvation, vermiculite and smectite exhibiting basal spacings of ∼14 and ∼18 Å, respectively, after such treatment.[1,47,48] However, distinct hydration behavior has not been reported for these two mineral species, and the predominance of bi-hydrated layers has been documented for the two species as a function of relative humidity. As a consequence, these two expandable 2:1 phyllosilicates will be considered together in the following.

For modeling XRD results of clay minerals containing 2W layers, the interlayer water configuration usually assumed for bi-hydrated smectite is that used for the calculations

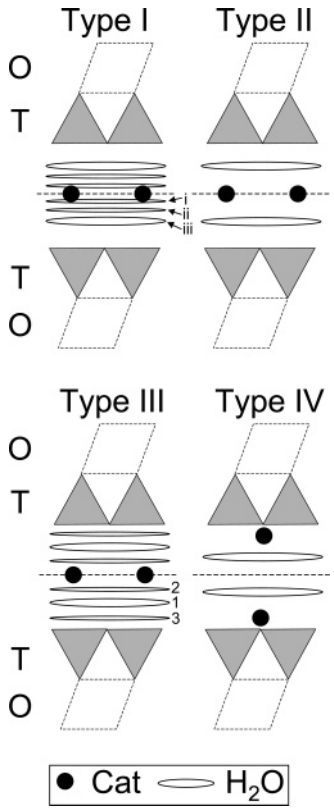

Figure 12. Schematic description of the different configurations proposed in the literature for interlayer species in 2W smectite layers. O and T refer to the octahedral and tetrahedral sheets of the 2:1 layer, respectively. Labels of the different sheets of H_2O molecules are detailed in the text.

showed in Figures 1a and 10 and already described (Type I, Figure 12).[1] This model does not allow the description of experimental XRD patterns (Figure 10) and may be rejected.

Most of the three-dimensional structural determinations of 2W interlayer configuration were actually performed on vermiculite as this mineral frequently exhibits ordered stacking sequences and because its higher content of interlayer cations allows for a more accurate refinement of cation positions as compared to smectite. In addition vermiculite, as illite, presents an ordered distribution of interlayer cations which eases the structural characterization of the interlayer configuration as compared to smectite.[49] The structural studies devoted to the configuration of interlayer species have led to different structure models that will be described below.

In bi-hydrated Mg-vermiculite, Mg^{2+} cations are located in the mid-plane of the interlayer with one sheet of H_2O molecules on each side of this plane (Type II, Figure 12).[5,50−53] According to this model, Mg is octahedrally coordinated by six H_2O molecules, whereas additional H_2O molecules, which are weakly bound to the cation, are located on the same plane as the six cation-bound H_2O molecules.[54−57]

(46) Bailey, S. W. *Clay Miner.* **1980**, *15*, 85−93.
(47) de la Calle, C.; Suquet, H. In *Hydrous Phyllosilicates (exclusive of micas)*; Bailey, S. W., Ed.; Mineralogical Society of America: Washington, DC, 1988; Reviews in Mineralogy Vol. 19, pp 455−496.
(48) Walker, G. F. *Clay Miner. Bull.* **1958**, *3*, 302−313.
(49) Besson, G.; Misfud, A.; Tchoubar, C.; Méring, J. *Clays Clay Miner.* **1974**, *22*, 379−384.
(50) Mathieson, A. M.; Walker, G. F. *Am. Mineral.* **1954**, *39*, 231−255.
(51) Mathieson, A. M. *Am. Mineral.* **1958**, *43*, 216−227.
(52) Bradley, W. F.; Serratosa, J. M. In *Clays & Clay Minerals, Proceedings of the 7th Clay Conference*; Pergamon Press: 1960; pp 260−270.
(53) Shirozu, H.; Bailey, S. W. *Am. Mineral.* **1966**, *51*, 1124−1143.
(54) Alcover, J. F.; Gatineau, L.; Méring, J. *Clays Clay Miner.* **1973**, *21*, 131−136.
(55) Alcover, J. F.; Gatineau, L. *Clay Miner.* **1980**, *15*, 25−35.
(56) Alcover, J. F.; Gatineau, L. *Clay Miner.* **1980**, *15*, 239−248.

Table 4. Structural Parameters of the Different Configurations Reported in the Literature for Interlayer Water in Bi-Hydrated Smectite Layers

Type I Configuration[a]

reference	sample	cation−$H_2O_{(iii)}$[b]	cation−$H_2O_{(ii)}$[b]	cation−$H_2O_{(i)}$[b]	B_{wat}[c,d]
Moore and Reynolds[1]	2W−smectite	1.20	1.06	0.35	11/2[§]

Type II Configuration

reference	sample	O_{layer}−H_2O[b]	cation−H_2O[b]	d_{001}[e]	nH_2O/nCat[f]	B_{wat}[c]
Mathieson et al.[51]	Mg−vermiculite	2.76	1.14	14.34		5.4
Shirozu et al.[53]	Mg−vermiculite	2.67[g]	1.17[g]	14.33	7.44	6.1
Alcover et al.[55]	Mg−vermiculite	2.69	1.19	14.36		
Le Renard et al.[60]	altered Ca−phlogopite	2.77	1.41	14.96	8.60	
	altered Na−phlogopite	2.71	1.43	14.87	10.70	
	altered Li−phlogopite	2.71	1.30	14.62	8.79	
Beyer et al.[59]	Na−vermiculite	2.70[g]	1.44[g]	14.85	4.00	3.9

Type III Configuration

reference	sample	O_{layer}−H_2O[b,h]	cation−-H_2O[b,h]	d_{001}[e]	nH_2O/nCat[f]	B_{wat}[c]
de la Calle et al.[61]	Ca−vermiculite	2.78	1.45[f]	14.92	7.34	5.5
Slade et al.[58]	Ca−vermiculite	2.82	1.41[f]	14.89	8.02	2.5
	Na−vermiculite	2.66	1.42	14.85	5.58	3.9

Type IV Configuration

reference	sample	O_{layer}−H_2O[b]	O_{layer}−Cation[b]	cation−H_2O[b]	d_{001}[e]	nH_2O/nCat[f]	B_{wat}[c]
Ben Brahim et al.[13]	Na−Beidellite	3.00	1.00	2.00	15.25	11.87	5

[a] Configurations of interlayer water in bi-hydrated smectite layers are schematized in Figure 12. [b] Distances are measured in projection along the c^* axis and given in Å. O_{layer}, H_2O, and cation stand for the outermost plane of oxygen from the 2:1 layer, the H_2O molecules, and the interlayer cations, respectively. [c] B_{wat} is the Debye−Waller temperature factor reported for H_2O molecules (in Å^2). [d] Debye−Waller factor is 11 Å^2 for plane iii and 2 Å^2 for planes i and ii, respectively. [e] Basal distance d_{001} along the c^* axis is given in Å. [f] nH_2O/nCat represents the ratio between the number of interlayer H_2O molecules and that of interlayer cations. [g] Average value for the different planes of H_2O molecules. [h] Distances are given for the denser plane of H_2O molecules.

A Type II configuration of H_2O molecules was also proposed for Na-saturated vermiculite,[58,59] and for Na-, Ca-, and Li-rich altered phlogopites.[60]

A second configuration of interlayer species has been proposed for Ca-saturated vermiculites (Type III, Figure 12).[58,61,62] In this model, two distinct coordinations are reported for Ca^{2+} cations, with two out of three Ca^{2+} cations being octahedrally coordinated as in type II configuration, whereas remaining Ca^{2+} cations exhibit a cubic coordination. This dual coordination induces the presence of two discrete planes of H_2O molecules (planes 2 and 3, Figure 12) in addition to that observed in the type II configuration, which holds most H_2O molecules (plane 1, Figure 12). The increased heterogeneity of H_2O configuration in Ca-, Sr-, and Ba-saturated samples as compared to Mg-saturated ones was confirmed both from diffraction and IR results.[56,57] A Type III configuration of H_2O molecules was also proposed for Na-saturated vermiculite.[58] Figure 13 compares the 2WG configuration of interlayer H_2O molecules determined for Ca−SWy-2 (40% RH) in the present study with that reported in the literature for Ca-saturated vermiculite.[58,61] After normalization of the three distributions to the denser plane of H_2O molecules, the three planes of H_2O molecules appear closely related to the 2WG configuration proposed in the present study to describe the positional distribution of interlayer species.

To compare the Δd values obtained in the present study with those reported in the literature (1.14−1.45 Å, Table 4), these values can be normalized to the thickness of the interlayer space to better account for the balance of the interactions with the interlayer cation on one hand and the 2:1 layer on the other hand (Table 5). Following such a normalization procedure, the Δd values determined for the 2WG configuration of H_2O molecules are consistent with those reported in the literature, whereas lower values are obtained when assuming a 2WS configuration.

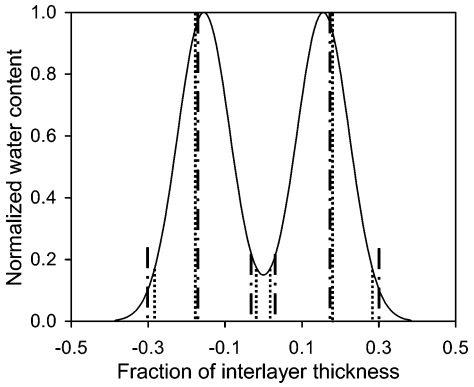

Figure 13. Comparison of the distributions of H_2O molecules reported for bi-hydrated smectites. The distributions are normalized to the denser plane of H_2O molecules, and z-coordinates are given in fraction of the interlayer with the origin located in the interlayer mid-plane thickness.The distribution determined from XRD profile modeling for the Ca-saturated SWy-2 montmorillonite sample (40% RH) is plotted as a solid line, whereas data from de la Calle et al. (ref 58) and from Slade et al. (ref 61) are shown as dashed and dotted-dashed lines, respectively.

(57) Fornés, V.; de la Calle, C.; Suquet, H.; Pezerat, H. *Clay Miner.* **1980**, *15*, 399−411.
(58) Slade, P. G.; Stone, P. A.; Radoslovitch, E. W. *Clays Clay Miner.* **1985**, *33*, 51−61.
(59) Beyer, J.; Graf von Reichenbach, H. *Clay Miner.* **2002**, *37*, 157−168.
(60) Le Renard, J.; Mamy, J. *Bull. Groupe Franç. Argiles* **1971**, *23*, 119−127.
(61) de la Calle, C.; Pezerat, H.; Gasperin, M. *J. Phys.* **1977**, *C7*, 128−133.
(62) de la Calle, C.; Suquet, H.; Dubernat, J.; Pezerat, H. *Clay Miner.* **1978**, *13*, 275−197.

Table 5. Distances along the *c Axis between the Interlayer Mid-Plane and the Maximum Density of the H_2O Molecule Distribution normalized to the Thickness of the Interlayer Space for the Different Configurations of Interlayer Species**

sample	2WS $B_{wat} = 2$[a]	2WS $B_{wat} = 11$[a]	2WG[b]
Ca−SWy-2 (40%RH)	27.8%[c]	30.1%	31.0%
Ca−SWy-1 (80%RH)	26.8%	29.4%	30.5%
Sr−SWy-1 (60%RH)	26.7%	29.4%	31.1%
Sr−SWy-1 (80%RH)	26.1%	30.7%	33.1%
Na−SWy-2 (80%RH)	26.7%	31.4%	33.4%
Na−$Sap_{0.8}$ (90%RH)	27.1%	30.0%	31.4%
Na−$Sap_{1.4}$ (90%RH)	28.4%	31.4%	31.9%
mean value	27.1% ± 0.7%	30.3% ± 0.8%	31.8% ± 1.0%
literature mean value[d]		32.7% ± 2.1%	

[a] 2WS corresponds to an interlayer configuration of H_2O molecules distributed as one plane on either side of the interlayer mid-plane. The Debye−Waller temperature factor for water (B_{wat}) is given in Å^2. [b] 2WG corresponds to an interlayer configuration of H_2O molecules distributed according to a Gaussian function on either side of the interlayer mid-plane. [c] The distance along the *c** axis between the interlayer mid-plane and the maximum density of the H_2O molecule distribution (Δd) is normalized to the thickness of the interlayer (layer thickness minus the thickness of the 2:1 layer, 6.54 Å). [d] Average value calculated from the data reported for Type II and Type III configurations of interlayer species (refs 51, 53, 55, and 58−61).

In addition, *z*-coordinates along *c** axis were recalculated together with typical distances between the 2:1 layer and the planes of H_2O molecules, and between H_2O molecules and interlayer cations (Table 4). For type II and III configurations the distance between the 2:1 layer and the densest plane of H_2O molecules scatters between 2.36 and 2.82 Å and is consistent with the formation of H-bonds between interlayer H_2O molecules and the clay framework. The distance between the densest plane of H_2O molecules and the interlayer cation ranges from 1.14 to 1.45 Å.

Specific Interlayer Structure Resulting from the Presence of Tetrahedral Substitutions. A third configuration of water in 2W smectite has been envisaged for Na-beidellite samples, with Na^+ cations being partly engaged in the ditrigonal cavities of the 2:1 layers and the coordinated H_2O molecules distributed on either side of the interlayer mid-plane which is devoid of atoms (Type IV, Figure 12).[12,13,63] Such a migration of the interlayer cation from the interlayer mid-plane toward the 2:1 clay framework is consistent with MC simulations and IR spectroscopy results which both support the formation of inner-sphere complexes for monovalent

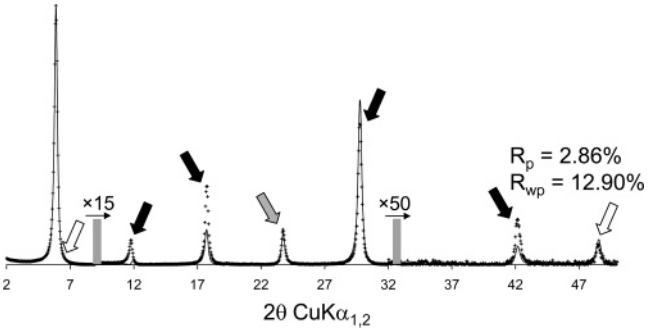

Figure 14. Comparison between experimental and calculated XRD patterns for the Na-saturated $Sap_{1.4}$ saponite sample recorded at 90% RH. Structural parameters used for the calculations are listed in Tables 1, 2, and 3. Patterns as for Figure 1. Calculation is performed assuming a Type IV configuration of interlayer species with a shift of the interlayer cation from the interlayer mid-plane toward the 2:1 clay framework (ref 13).

cations in tetrahedrally substituted 2:1 phyllosilicates.[21,24,26,31] In the present study, similar distributions of interlayer species have been determined whatever the location of the layer charge deficit in agreement with previous reports of Type II and Type III configurations of interlayer species in tetrahedrally substituted 2W vermiculites.[58−60] The central location of Na^+ cations was found to be consistent with experimental XRD data even when Na^+ cations account for a significant part of the interlayer electronic density (13% of the interlayer electrons for sample Na−$Sap_{1.4}$). Furthermore, if a Type IV configuration is assumed for the distribution of interlayer species, significant discrepancies arise between experimental and calculated patterns, especially for the 002 and 003 reflections which are extremely sensitive to the presence of interlayer species at the interlayer mid-plane position (Figure 14). In conclusion, the present data do not provide experimental evidence for the migration of monovalent cations toward the surface of tetrahedrally substituted 2:1 layers.

Acknowledgment. The results presented are a part of a Ph.D. thesis granted by Andra (French National Agency for Nuclear Waste Disposal). Andra is thanked for the permission to publish this manuscript and for financial support. B.L. acknowledges financial support from the CNRS/PICS709 program, and from the CNRS/SdU "postes rouges" fellowships granted to B.A.S. V.A.D. and B.A.S. are grateful to the Russian Science Foundation for partial financial support. Laurent Michot (LEM, Nancy, France) is thanked for the fruitful discussions about smectite hydration. Jean-Louis Robert (IST Orléans, France) kindly provided the synthetic saponite samples.

CM047995V

(63) Ben Brahim, J.; Armagan, N.; Besson, G.; Tchoubar, C. *J. Appl. Crystallogr.* **1983**, *16*, 264−269.